Electronic Supplementary Material (ESI) for Journal of Materials Chemistry C.

Supplementary Information

Diffusion of Brønsted Acidic Dopants in Conjugated Polymers

Phong H. Nguyen,[a] Michael Schmithorst,[a] Thomas E. Mates,[c] Rachel A. Segalman [a,b,c] Michael L. Chabinyc[c]

[a]*Department of Chemical Engineering, University of California, Santa Barbara, California 93106, USA*
[b]*Department of Chemistry and Biochemistry, University of California, Santa Barbara, California 93106, USA*
[c]*Materials Department, University of California, Santa Barbara, California 93106, USA*

Contents

Experimental Methods

P3HT Film Preparation

P3HT (74 kDa, 2.2 PDI, 96% regioregular) was purchased from Rieke Metals. Solutions were made by dissolving P3HT in 1:1 (v:v) chlorobenzene:dichlorobenzene, stirred overnight at 120 °C in an N_2 glovebox. Solutions were cooled to room temperature and filtered through 0.45 μm PTFE filters prior to spin-casting. For GIWAXS and XPS/DSIMS samples, native oxide silicon substrates were cleaved from wafers and cleaned by sequential sonication in acetone, DI water, and isopropanol. UV-vis substrates were cut from thin quartz coverslips to fit in standard 1 cm quartz cuvettes and cleaned using the same procedure. For conductivity measurements, 15 × 15 mm quartz substrates were cleaned using the same procedure. After drying, substrates were plasma cleaned with 300 mTorr of air at 100 W, then immersed in isopropanol until immediately before spin casting. Thin (10 ± 2.4 nm thick) films were made by spin casting 5 mg/mL P3HT (in 1:1 chlorobenzene:dichlorbenzene) at 3,000. Thicker (265 ± 11 nm thick) films were spun from 35 mg/mL solutions at 1,000 RPM. Subsequently, all samples were annealed in N_2 at 120 °C for 30 minutes.

Immersion Doping Procedure

Doping solutions were made by dissolving HTFSI (trifluoromethanesulfonimide, Sigma Aldrich) in either CD_3OD (166.2 mM, 5 wt% HTFSI) or CH_3OH (148.3 mM, 5 wt% HTFSI) in a N_2-filled glovebox and stirred overnight. Immersion doping was performed either in a fume hood or in an N_2-filled glovebox (samples exposed to air are noted explicitly throughout) by immersing P3HT films in 20 to 40 mL of dopant solution, and removed and dried after 3 hours, 1 day, and 2 days. Samples were further dried in high vacuum conditions (10^{-8} torr, ambient temperature) overnight prior to analysis. For DSIMS samples, deuterated polystyrene (polystyrene-d8) D calibration and polystyrene (polystyrene) spacing layers are added by floating spun cast polystyrene and polystyrene-d8 films from quartz substrates onto water. The polystyrene and polystyrene-d8 films are lifted from the water bath using an O-ring, left to dry for 5 minutes, and overlaid onto the doped P3HT films to be depth profiled. After, samples were further dried overnight (10^{-8} torr, ambient temperature) prior to depth profiling.

In Situ UV-Vis Spectroscopy

Film samples were placed in standard solution cuvettes such that the film surface was oriented towards the light source. Cuvettes fit with septum caps were filled with N_2-blanketed doping solutions and scans ranging from 190 nm to 1100 nm were acquired up to 4320 minutes (3 days). All UV-vis spectra were acquired using an Agilent Technologies Cary 60 UV-vis spectrometer and data analysis was conducted using custom MATLAB scripts. Polaron absorbance was tracked by subtracting the first spectra from all others to create difference spectra. The primary polaron absorbance and 0-1 vibronic absorbance at 1.55 eV and 2.23 eV, respectively, were tracked over time to extract doping reaction kinetics.

Conductivity Measurements

For four-point probe conductivity measurements, shadow mask evaporation was used to deposit 30 nm gold electrodes (1 mm width, 0.2 mm length) using an Angstrom Engineering metal evaporator. Measurements were performed under inert N_2. Current ranging from 100 to -100 μA, was supplied using a Keithley 6220 precision current source and voltage was measured using a Keithley 2400 source meter. Reported conductivities are the average of two measurements on each sample.

UV-Visible Spectroscopy and Fitting Kinetic Models

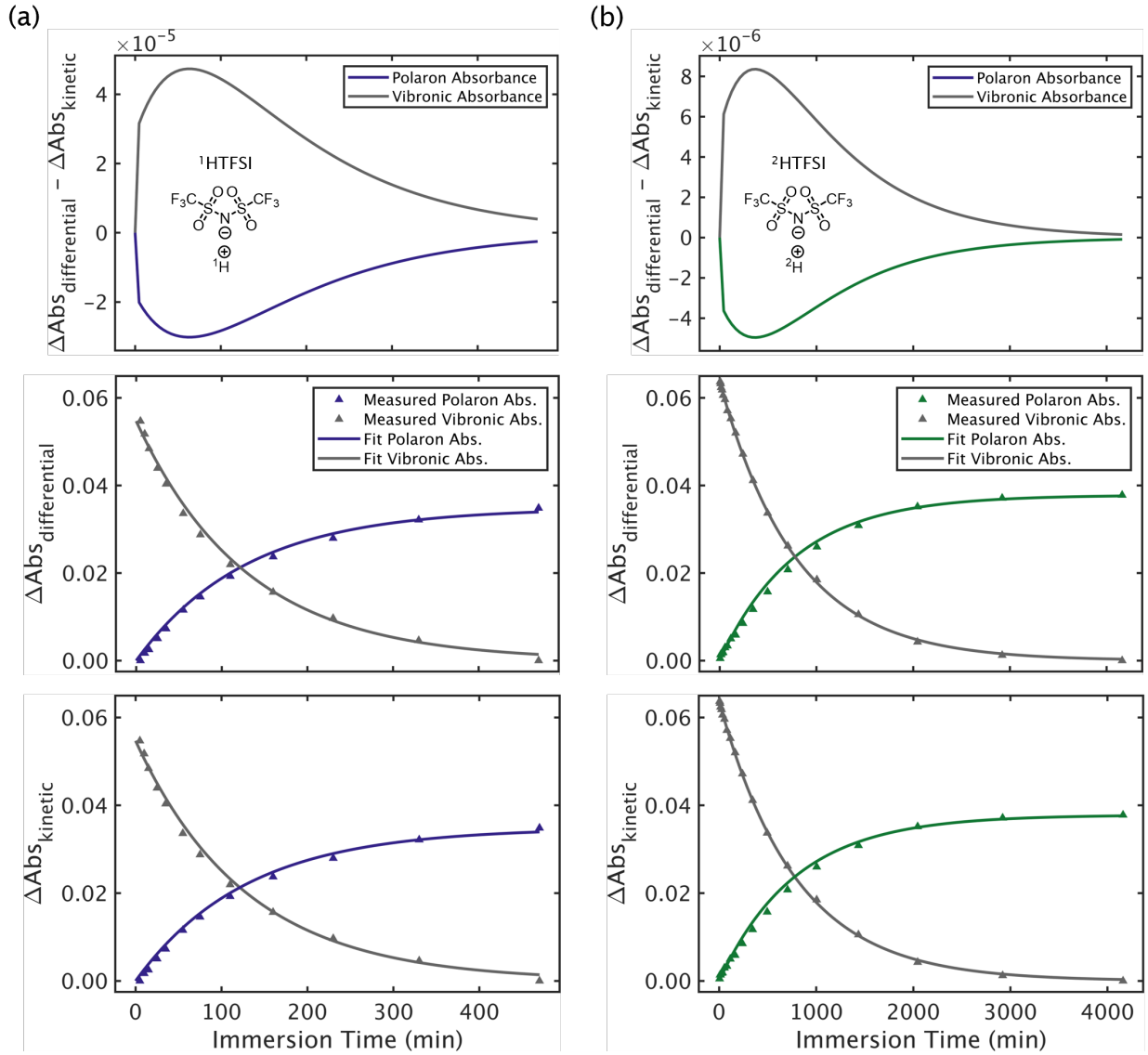

Fig. S1 (a) (Top) Differences between fit of the diffusion-reaction equation (Equation 5) ($\Delta Abs_{differential}$, middle) and differential mole balances (Equations 8 and 9) ($\Delta Abs_{kinetic}$, bottom) for 10 nm P3HT films in (a) HTFSI (CH_3OH) and (b) DTFSI (CD_3OD) solutions.

Depth Profiling Quantification

Immersion-doped samples were cleaved in two for concurrent XPS and DSIMS depth profiling measurements. Additional polystyrene and deuterated polystyrene layers were floated onto DSIMS samples to provide deuterium calibration standards. F 1s atomic percentage was quantified from XPS depth profiles using the Avantage software suite provided by Thermo Fisher Scientific Inc. A complete XPS depth profile was taken for one sample to calibrate the etch time with etch depth using the known P3HT film thickness. Similarly, DSIMS depth profiles were converted from

sputtering time to depth using the known P3HT film thickness. Least-squares fitting was performed to scale the ^{19}F DSIMS profile to the F 1s XPS depth profile. All samples demonstrated good agreement between the XPS and SIMS fluorine profiles (**Fig. S2**). The XPS F 1s signal approaches the noise floor after approximately 1 atomic % at the survey scan conditions employed, corresponding to a noise floor of approximately 10^{20} cm^{-3} and depth of 30 nm.

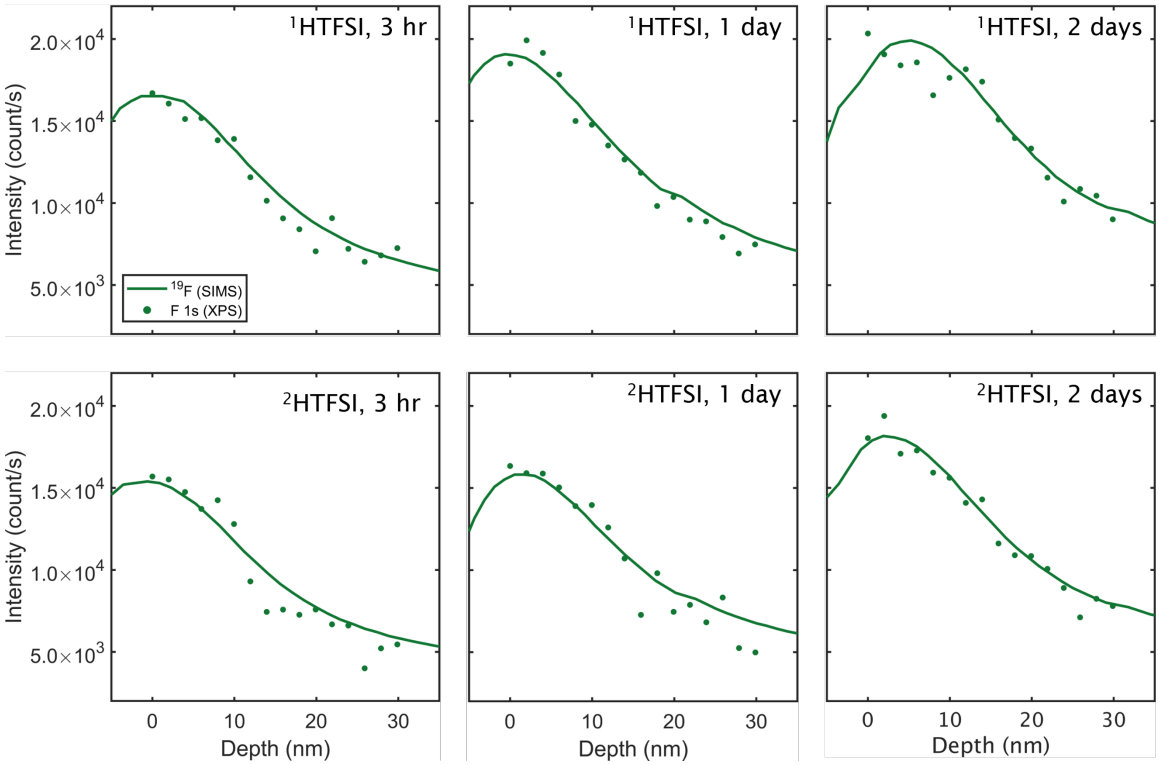

Fig. S2 Matching ^{19}F and F 1s profiles from XPS and DSIMS depth profiling, respectively, for samples whose dopant uptake are summarized in **Fig**. **7** of the main text. All samples were exposed to air during the doping process.

The F 1s peak is quantified at each depth, allowing for the ^{19}F profile to be scaled accordingly using least squares fitting. Resulting depth profiles retain high depth resolution and signal-to-noise ratio while being stoichiometrically calibrated. Reported total D and $TFSI^-$ follow from integrating concentration depth profiles through the 265 nm P3HT region and accounting for the 3.1×10^{-5} cm^2 regions analyzed by DSIMS. Model results (presented in **Fig. 7** of the main text) are scaled in the same way for direct comparison with experimental results.

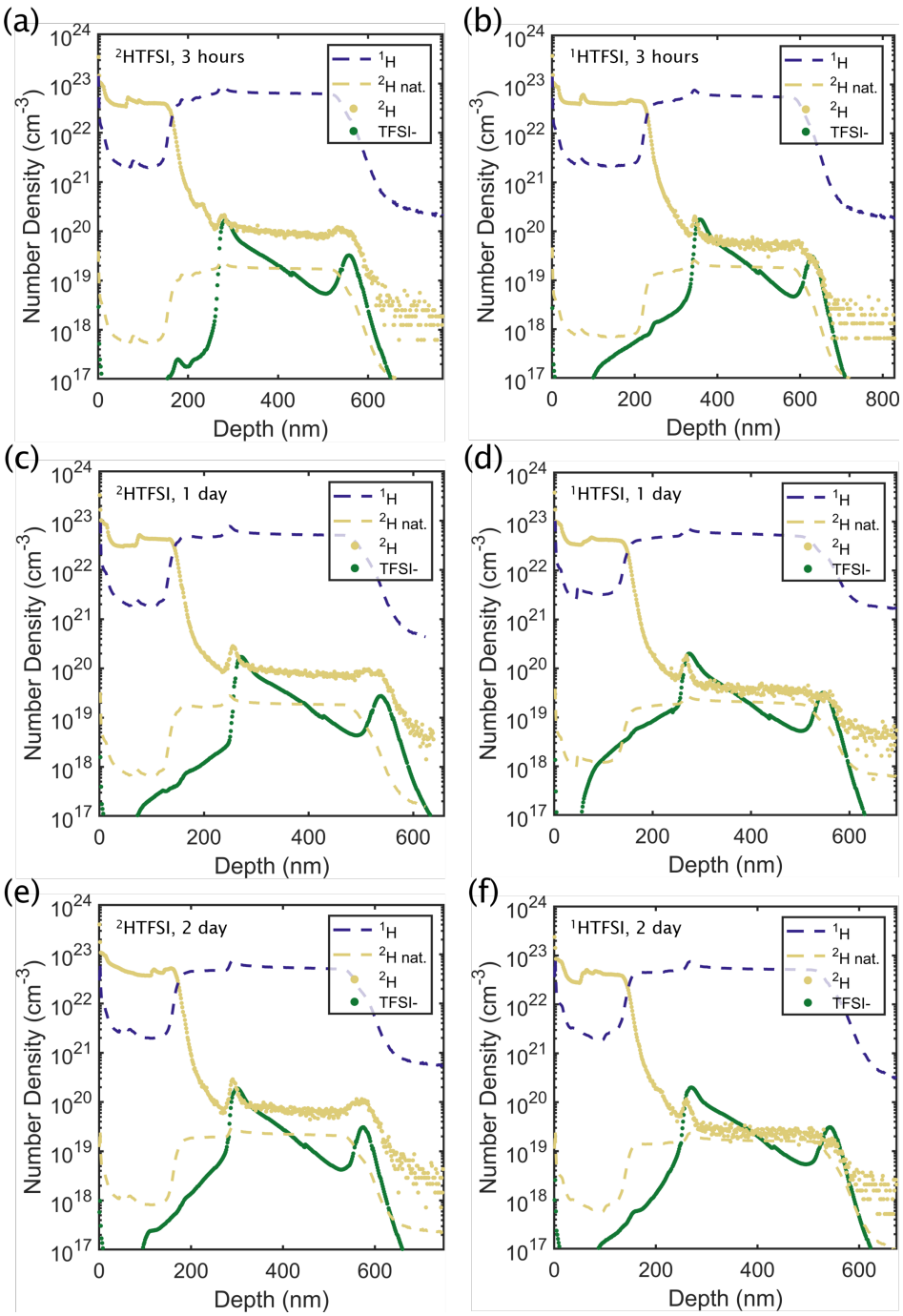

Fig. S3 Concentration depth profiles of P3HT films immersion doped in in DTFSI (left column) and HTFSI (right column) solution 3 hours (a, b), 1 day (c, d), and 2 days (e, f), corresponding to dopant uptake measurements summarized in **Fig. 7** of the main text. All samples presented here were exposed to air during the doping process.

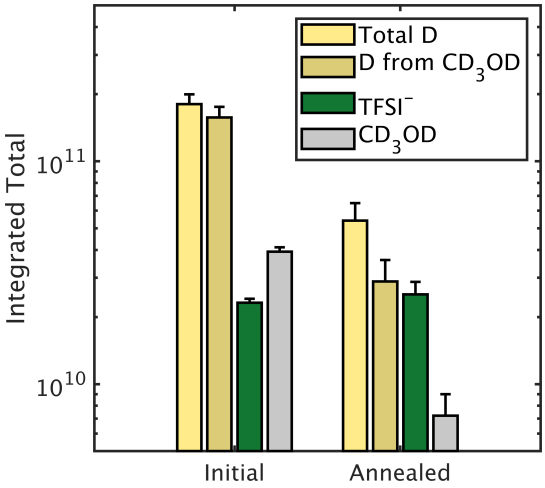

Fig. S4 Integrated D and $TFSI^-$ throughout 265 nm P3HT films immersion doped in DTFSI solution. Error bars correspond to one standard deviation (N = 2).

The integrated concentration of D throughout the P3HT film (light yellow bar) exceeds the amount of $TFSI^-$ (green bar) by approximately an order of magnitude before annealing [$(1.8 \pm 0.2) \times 10^{11}$ vs $(2.3 \pm 0.9) \times 10^{10}$, respectively]. The D attributable to CD_3OD (dark yellow bar) can be estimated by assuming the fraction of D originating from the doping reaction is equivalent to the amount of $TFSI^-$ at most. Normalizing the remaining D provides an estimate of residual CD_3OD content relative to $TFSI^-$. Most of the residual CD_3OD evaporates during annealing which suggests that D imparted by the doping reaction constitutes a significant fraction of the D signal after annealing.

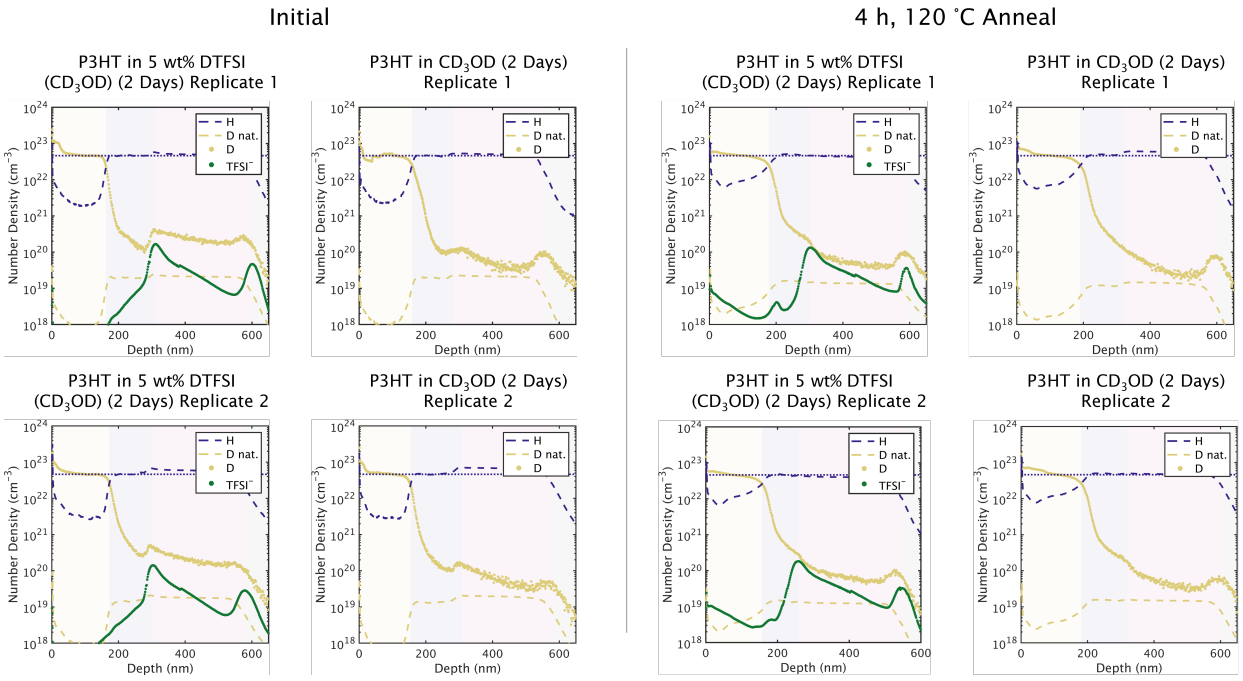

Fig. S5 Concentration depth profiles of P3HT films immersed in DTFSI (CD_3OD) solution and in CD_3OD solvent only. DTFSI-doped samples show significant D enrichment as compared to controls samples immersed only in CD_3OD solvent (left). While most of the D disappears following the annealing process (right), residual D remains primarily at the P3HT top surface for both DTFSI-doped and control samples.

A majority of the D enrichment from resulting from the doping process is attributable to residual CD_3OD solvent (**Fig. S5**). The annealing process removes most of the residual CD_3OD; however, a significant amount relative to $TFSI^-$ remains. While both annealed DTFSI-doped and control samples exhibit D-enrichment, the DTFSI-doped sample is significantly D-enriched throughout the film depth as compared to control samples. This suggests that excess D comes from the doping reaction.

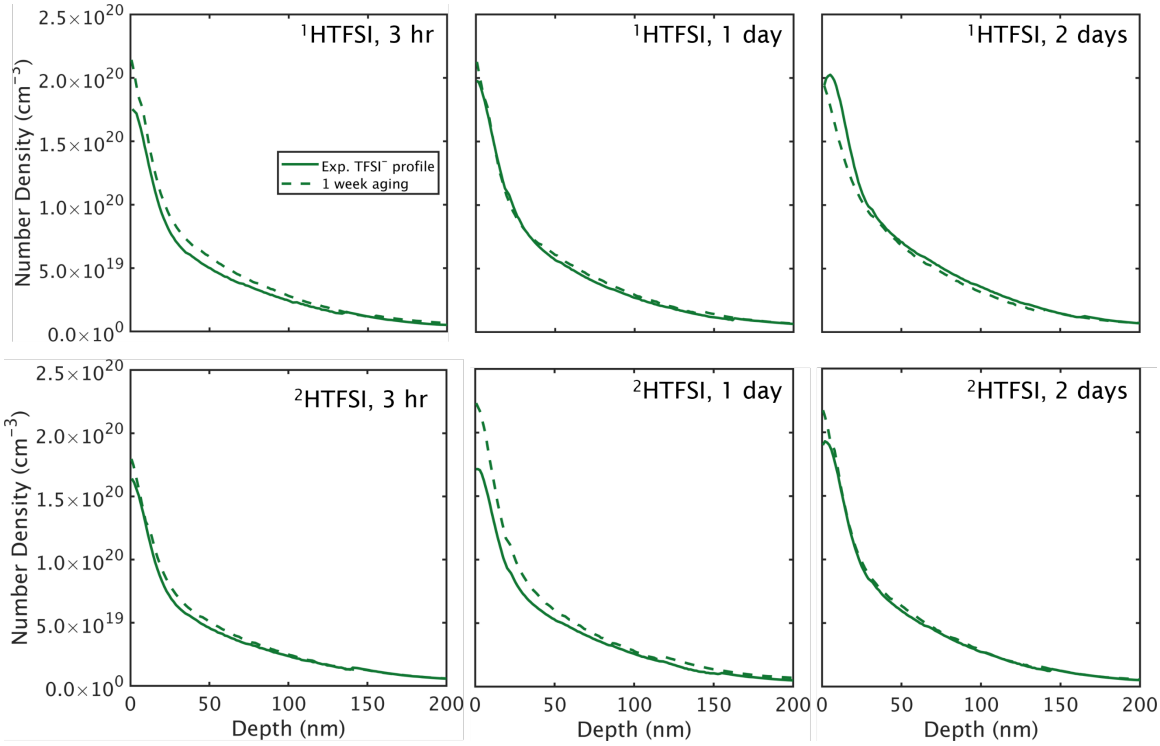

Fig. S6 Effect of sample aging for 1 week. The same samples as reported in **Fig. 7** were measured using complementary XPS and DSIMS depth profiling.

The quantified depth profile after 1 week of aging in an inert atmosphere at ambient temperature shows that $TFSI^-$ diffusion does not occur significantly within the 1-week time frame from sample doping to sample measurements. Deviations between the $TFSI^-$ profiles of the samples as reported and after 1 week are below the interfacial resolution of the technique.

CP/MAS NMR of P3HT Co-Processed with HTFSI

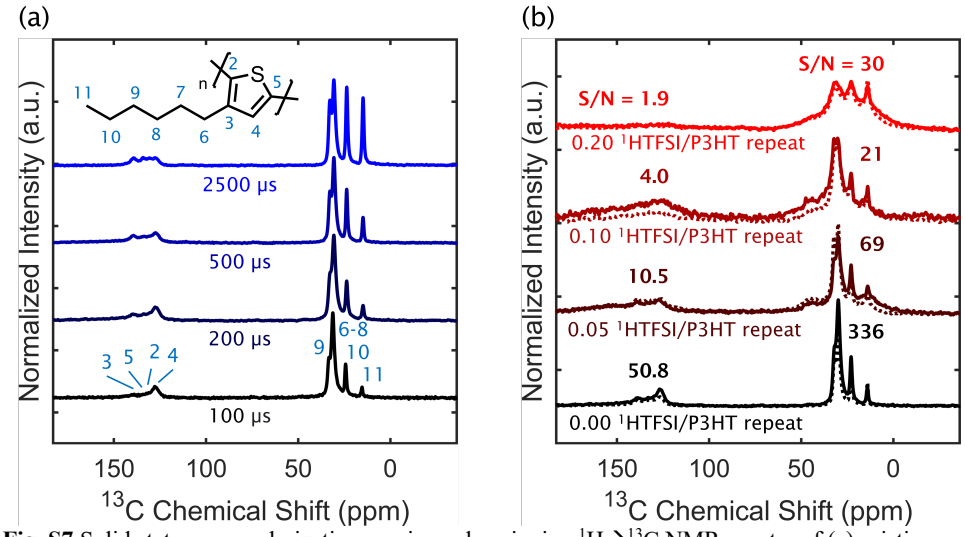

Fig. S7 Solid state cross-polarization magic angle spinning $^1H \rightarrow {}^{13}C$ NMR spectra of (a) pristine and (b) HTFSI-doped P3HT. (a) Decreasing the cross-polarization contact time between ^1H and ^{13}C highlights carbons in proton-abundant environments. There is only one native proton on the P3HT backbone (position 4, P3HT repeat unit labeled on the inset) whose position is highlighted at

short contact times. (b) Cross-polarization at short (200 μs) and long (500 μs) contact times for P3HT:HTFSI at different dopant to polymer repeat unit ratios. Signal-to-noise (S/N) ratios (for 200 μs contact time experiments, labeled aromatic and aliphatic regions) decrease with increasing dopant to polymer repeat unit ratios.

$^{1}H \rightarrow {}^{13}C$ cross-polarization magic-angle-spinning NMR experiments were performed on a 500 MHz Bruker Avance NMR Spectrometer equipped with a double-resonance 4 mm NMR probe at a magnetic field strength of 11.7 T and a MAS frequency of 10 kHz. For the pristine P3HT sample, 4096 scans were acquired with cross-polarization contact times of 100, 200, 500, and 2500 μs. For the HTFSI-doped P3HT samples of varying dopant levels, CP/MAS experiments with 200 μs and 500 μs contact times were acquired. For the 0.05 HTFSI/P3HT sample, 8192 scans were acquired, and for the 0.10 and 0.20 HTFSI/P3HT samples 16384 scans were acquired in order to observe signals above the noise level in the aromatic ^{13}C NMR spectrum region. The signal-to-noise (S/N) ratios listed in Fig. S2b are normalized to 16384 scans for each sample for the purpose of comparison. A recycle delay of 1 s was used for all experiments, and SPINAL64 ^{1}H heteronuclear decoupling was applied during acquisition.

In the CP/MAS contact time experiment, polarization is transferred from abundant ^{1}H to ^{13}C to enhance signal. The length scale of polarization transfer varies with time; short contact times are able to highlight carbons in proton-rich environments. For any significant acidic proton retention, the proton is expected to bond to the P3HT backbone; however, CP/MAS NMR of HTFSI-doped P3HT does not unambiguously indicate additional protons added to any potential bonding sites (see **Fig. S7**). Here, we also note that the signal-to-noise ratio decreases with increasing HTFSI/P3HT repeat ratio due to increasing concentration of paramagnetic species (the hole-radical polaron). Paramagnetic species can prematurely relax polarization, reducing polarization transfer from ^{1}H to ^{13}C and leading to lower signal-to-noise ratios. Because of this, the CP/MAS NMR of highly doped P3HT cannot conclusively indicate whether protons are added, even for scans spanning several hours.

Angle-Resolved GIWAXS

X-ray scattering was performed at experimental station 11-3 at the Stanford Synchrotron Radiation Lightsource using an X-ray energy of 12.7 keV. Angle-resolved GIWAXS scans were acquired with 100 second exposures at each incidence angle from 0.05° to 0.13° in increments of 0.0025°. During the acquisition, samples were continuously rocked in the direction perpendicular to the X-ray flux by ± 2 mm around the sample center to mitigate beam damage.

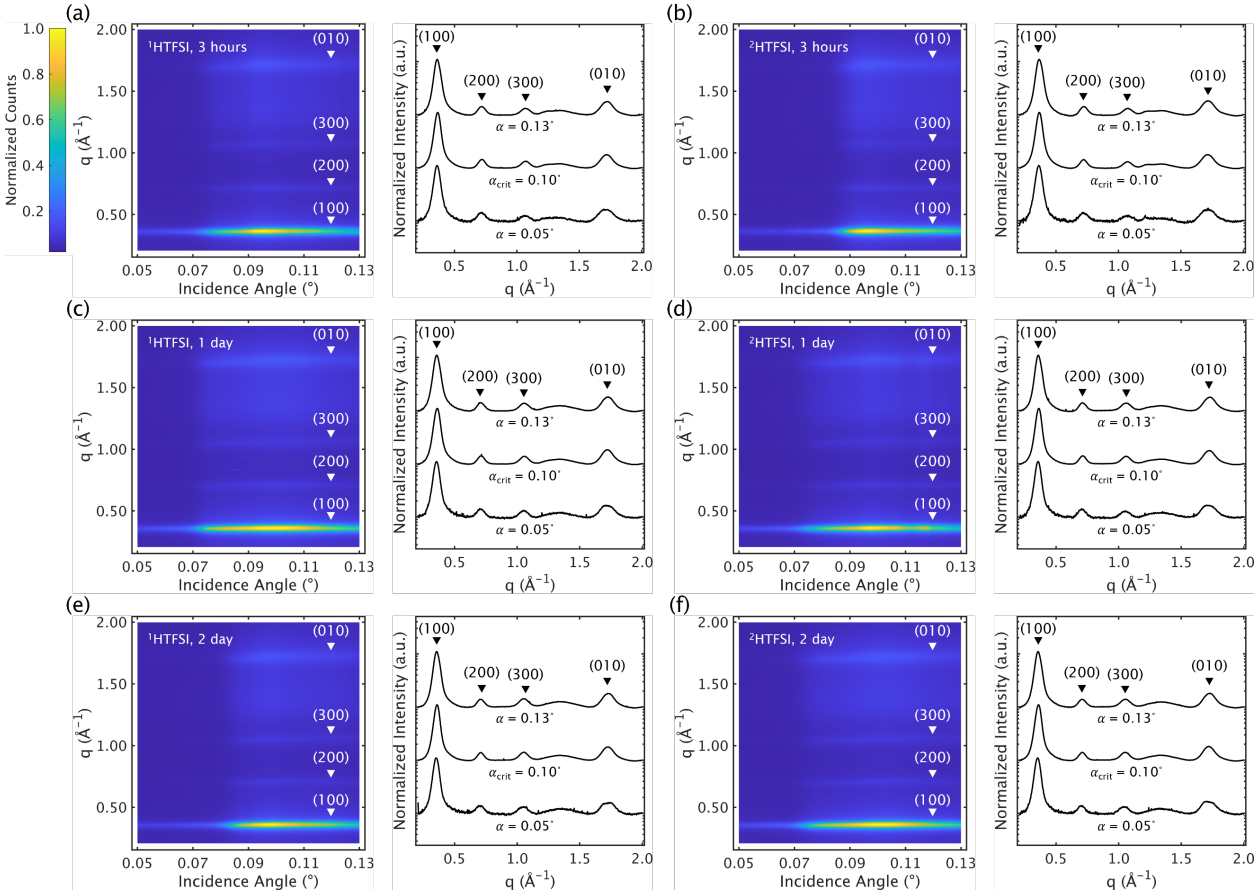

Fig. S8 Angle-dependent GIWAXS of 265 nm P3HT immersion-doped in HTFSI solution (exposed to air) (a, c, e) and DTFSI solution (also exposed to air) (b, d, f) for 3 hours, 1 day, and 2 days. All samples exhibited an expanded (100) stacking distance and two peaks near 3.7 Å (1.7 Å^{-1}) at shallow incidence only, indicative of surface doping.

Table S1. (100) stacking distances extracted from radially integrated GIWAXS data. (100) stacking distances are extracted from the average of the (100), (200), and (300) stacking distances. The reported (100) stacking distance is then the average of these at angles probing only the surface (incidence angle of 0.05° to 0.09°) and the film entirely/bulk (0.11° to 0.13°). Fitting is performed by subtracting background for each scan and least-squares fitting a Voigt line shape to (100), (200), (300), (020) and amorphous scattering using a custom MATLAB script.

Dopant Solution	Immersion Time	Surface (100) stacking distance (Å)	Standard Deviation	Bulk (100) stacking distance (Å)	Standard Deviation	Average Difference
Undoped	None	16.18	0.04	16.15	0.05	0.03
HTFSI	3 hours	17.58	0.05	17.4	0.019	0.16
HTFSI	24 hours	17.89	0.41*	17.7	0.080	0.24
HTFSI	48 hours	17.86	0.03	17.7	0.016	0.17
DTFSI	3 hours	17.45	0.02	17.3	0.008	0.11
DTFSI	24 hours	17.76	0.06	17.6	0.022	0.17
DTFSI	48 hours	17.91	0.03	17.7	0.020	0.23

*Larger standard deviation attributed to stray cosmic radiation striking the X-ray detector (zinger), visible in the detector image.

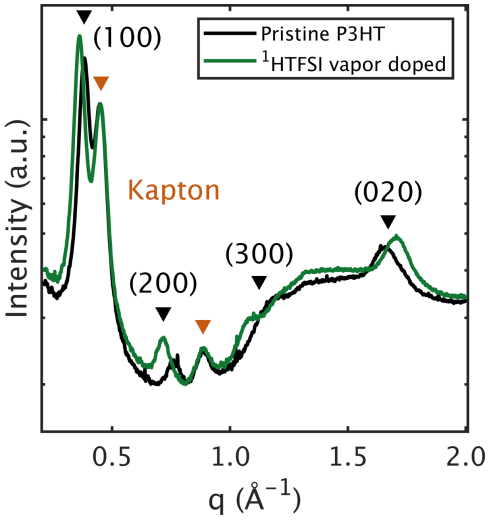

Fig. S9. Radially integrated scattering peaks from GIWAXS measurements of P3HT films doped with HTFSI from the vapor phase. Data is taken at a grazing incidence angle of 0.13°, corresponding to the entire thickness of the film. Additional scattering peaks are from Kapton used to seal the scattering cell and are used for intensity normalization. Upon doping, the alkyl spacing shifts from 0.38 $Å^{-1}$ (16.5 Å) to 0.36 $Å^{-1}$ (17.5 Å), while the π-π stacking shifts from 1.66 $Å^{-1}$ (3.8 Å) to (1.70 $Å^{-1}$) (3.7 $Å^{-1}$).

Roughness of Pristine and DSIMS-Profiled Films from Atomic Force Microscopy

To assess whether DSIMS signal broadening throughout the depth was likely due to beam damage, atomic force micrographs were measured for pristine and doped P3HT films (see **Fig. S10** and **Fig. S11**). Alignment of rows was performed using third-order polynomials. In both measurements, the sputtered surface is smoother than the pristine surface as quantified by the roughness average. While a rougher surface may be a byproduct of the immersion-doping process, these results also suggest that the elemental concentration profiles did not appreciably broaden due to beam damage.

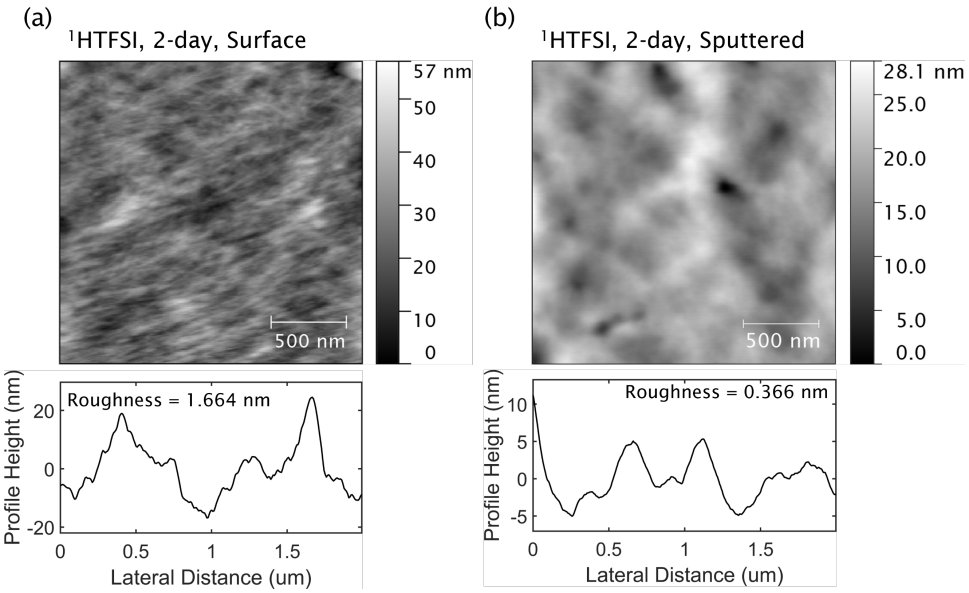

Fig. S10 Atomic force micrographs of pristine (a, top) and O_2^+-sputtered HTFSI immersion-doped P3HT films (b, top). Height profiles across micrograph midpoints show that depth profiling does not promote roughening of the sputtered surface. This suggests that sputtering-induced damage is not likely to cause broadening of the DSIMS depth profiles.

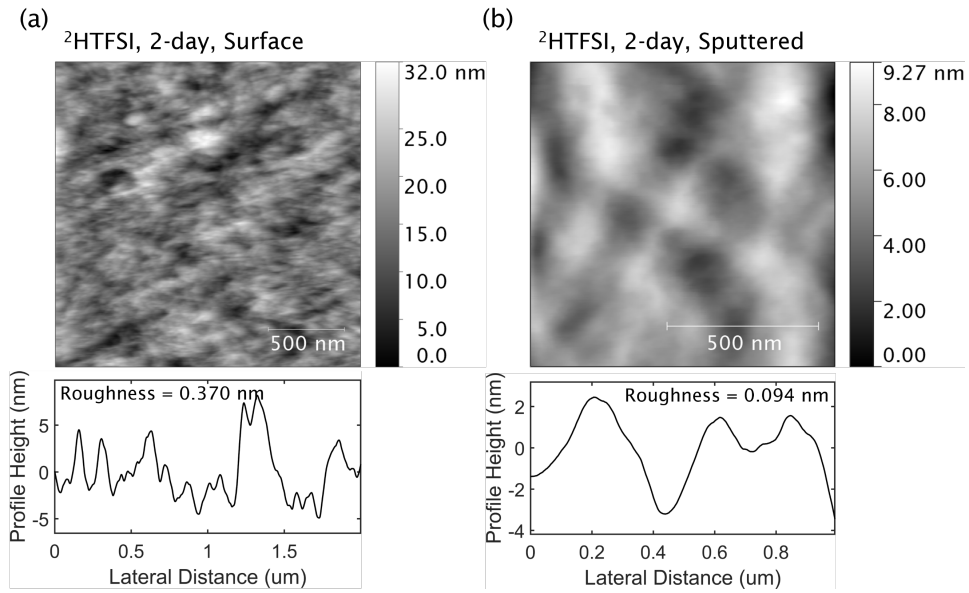

Fig. S11 Atomic force micrographs of pristine (a, top) and O_2^+-sputtered DTFSI immersion-doped P3HT films (b, top). Height profiles across micrograph midpoints show that depth profiling does not promote roughening of the sputtered surface. This suggests that sputtering-induced damage is not likely to cause broadening of the DSIMS depth profiles.